Progress In Electromagnetics Research C, Vol. 136, 75–86, 2023

Asymmetric Flare Shape Patch MIMO Antenna for Millimeter Wave 5G Communication Systems

Jetendra Jakhar[1], Tejpal Jhajharia[2, *], and Bharat Gupta[3]

Abstract—Today's 5G wireless communication evolution system demands millimeter wave frequency range antenna for its uses in several communication device applications. A 2-port Asymmetric Flare-Shape Patch Multiple Input Multiple Output (MIMO) antenna for mm-wave communication system is designed and presented. The antenna structure is constructed on a Rogers RT Duroid 5880 dielectric substrate with 1.6 mm thickness, 2.2 dielectric constant, and 0.0009 loss tangent. The constructed MIMO structure has an overall size of $26 \times 19.2\,\text{mm}^2$. The proposed MIMO design has -10 dB return loss performance over a frequency range of 20–40 GHz with more than 20 dB isolation between antenna elements, which shows the low mutual coupling between antenna elements. The performance of the suggested MIMO antenna is reported in terms of return loss, gain, ECC, and radiation pattern. The simulated and measured MIMO antenna performance characteristics are in good agreement. The suggested design achieves more than 20 dB isolation and 8.17 dB gain with an ECC value lower than 0.0001, which meets the diversity performance of the MIMO design with two antenna elements. The proposed MIMO design is compact and the best choice for 5G mm-wave applications.

1. INTRODUCTION

Recently, 5G wireless communication has significant improvements to meet the high data rate applications over the cellular network. The latest wireless infrastructure is developing with a requirement of the high bandwidth applications over the existing network infrastructure. The 5^{th} Generation wireless technology includes the 5G NR sub-6 GHz in a lower frequency band and 5G new radio n257/n258/n260/n261 in the millimeter-wave (mm-wave) frequency band. Presently, 5G mm-wave band infrastructures are developing with 24.25–27.5 GHz, 27.5–28.8 GHz, 37–43.5 GHz, and 39 GHz in various countries [1]. In the present era, technological development in wireless communication systems focuses on Multiple-Input Multiple-Output (MIMO) systems. MIMO system makes reliable communication for 5^{th}-generation wireless applications [2]. In a MIMO system multiple antennas are mounted on a single printed circuit board (PCB) at the transmitter and receiver on both sides [3]. MIMO antenna technology provides high-quality of services for both indoor and outdoor environments. To present a good quality of services, MIMO antenna system is the safest candidate or channel solution for non-line of sight (NLOS) wireless communication [4]. MIMO system can improve the quality of wireless communication with a high data rate, without increasing the bandwidth and transmitted power. At present, MIMO antenna design primarily includes single antenna element, multiple antenna layouts, and mutual coupling analysis between antenna elements, and focuses on the evaluation of low-cost and high-performance designs.

5G mm-wave antennas are intended to operate in the millimeter wave frequency spectrum, also identified as the extremely high frequency (EHF) band and have a high gain to balance the free space

Received 30 March 2023, Accepted 28 July 2023, Scheduled 11 August 2023
* Corresponding author: Tejpal Jhajharia (tejpal4u@gmail.com).
[1] Department of Electronics and Communication Engineering, Shri JJT University, Churela, Rajasthan, India. [2] Department of Electronics and Communication Engineering, Manipal University, Jaipur, India. [3] Department of Electrical Engineering, Shri JJT University, Churela, Rajasthan, India.

propagation losses. Presently, most of the antenna research is centered on the 25 GHz, 28 GHz, 38 GHz, and 60 GHz bands with MIMO antenna designs [5].

Wang et al. [6] proposed a MIMO antenna for Ka band, which operated in the frequency range of 24 GHz to 39 GHz. The proposed antenna geometry was complex. Lee et al. [7] presented a Vivaldi end-fire antenna array design. The suggested antenna was designed with a 10-Layer printed circuit board, for 27.5–28.5 GHz frequency range. The suggested antenna had very high thickness and low operating frequency range. Malviya et al. [8] suggested a planner MIMO antenna design with four elements. The suggested design was fabricated with a low-cost FR-4 substrate with larger size for lower frequency band 1.66 GHz–2.17 GHz, and comparatively lower isolation in all four elements. Patel et al. [9] suggested an inverted-L shaped patch antenna for wideband MIMO applications. The proposed MIMO design offered an impedance bandwidth in the frequency band of 26–40 GHz, with 15 dB isolation, 6 dBi gain, and an envelope correlation coefficient (ECC) value of 0.02.

In MIMO antenna design, the radiating elements are closely proximate to achieve a compact design. The proximity of radiating elements and shared ground plane affects the antenna performance. Such performance degrading effects are jointly recognized as mutual coupling, which severely affects the radiation characteristics and diversity behavior of the antenna system [10]. The mutual coupling is reduced in MIMO antenna design by using asymmetric patch shape, Vivaldi structure, defective ground structures, and metamaterials [11].

In this communication, a simple design of the MIMO antenna is proposed with an asymmetric flare-shape patch structure for 5G mm-wave wireless communication system.

2. DESIGN STUDIES AND METHODS

The proposed two-element MIMO antenna with an asymmetric flared shape patch has been designed for wide bandwidth, high gain, and low losses. The two-element MIMO antenna has an overall size of $26 \times 19.2\,\text{mm}^2$ with a $50\,\Omega$ impedance feed. The suggested antenna is designed using CST Microwave Studio 2019. A Rogers RT5880 dielectric substrate with a thickness of 1.6 mm, a permittivity of 2.2, and a loss tangent of 0.0009 is used. The best antenna design objectives for essential operating frequency band (mm-wave), high gain, compactness, and desired antenna parameters, a single antenna element is designed, simulated, and optimized in CST Microwave Studio software. The single-element antenna design with compact size, low return loss, and wide bandwidth for mm-wave communication is designed, and the suitable optimized dimension parameters for the best antenna parameters results are shown in Fig. 1 and Fig. 2.

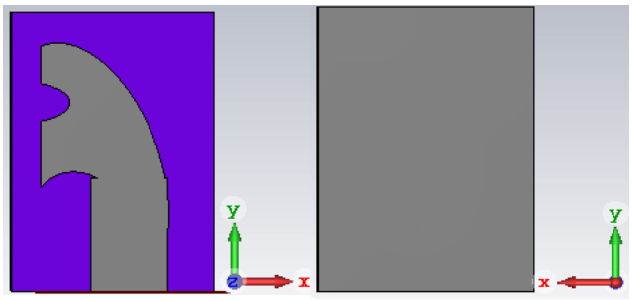

Figure 1. Schematic view of proposed single antenna.

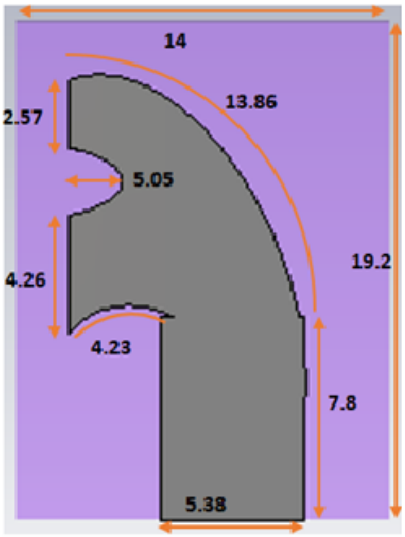

Figure 2. Dimension (in mm) of proposed single antenna.

2.1. Proposed Single Antenna Designing Steps

Initially, a flare-shaped patch of feed length $b = 7.8$ mm and feed width $a = 5.38$ mm in MGRID of CST of substrate Rogers RT5880 with dielectric constant 2.2, loss tangent 0.0009 for the frequency band of 20–40 GHz as shown in Fig. 3 design step-1(A-1) is designed. A 50 Ω impedance feed is applied at the feed point. The simulated −10 dB S_{11} impedance results are in the frequency ranges of 23–27 GHz and 29.56–40 GHz for design step-1(A-1). Further to improve the −10 dB S_{11} impedance results for the 20–40 GHz frequency range, a semi-oval shape slot of the dimension of 5.05 mm in depth and 2.57 mm down from the top of the flare-shape patch is removed as shown in design step-2(A-2). Secondly, a 4.23 mm arc shape slot is removed at the lower side of the patch near the feed line as shown in Fig. 3 in design step-3(A-3). With these amendments the simulated −10 dB impedance bandwidth covers the entire 20–40 GHz frequency band as shown in Fig. 4. The simulated results confirm the best-optimized dimension of the suggested single antenna design that provides good simulated S_{11} value at 25.5 GHz and 30 GHz as shown in Fig. 4. The 50 Ω impedance matching at 30.02 GHz frequency is shown in Fig. 5.

Figure 6 shows the simulated max gain over frequency plot of the suggested single-element antenna design. The simulated maximum gain is 8.14 dB at 38 GHz, and the minimum gain is 5.8 dB at 25 GHz,

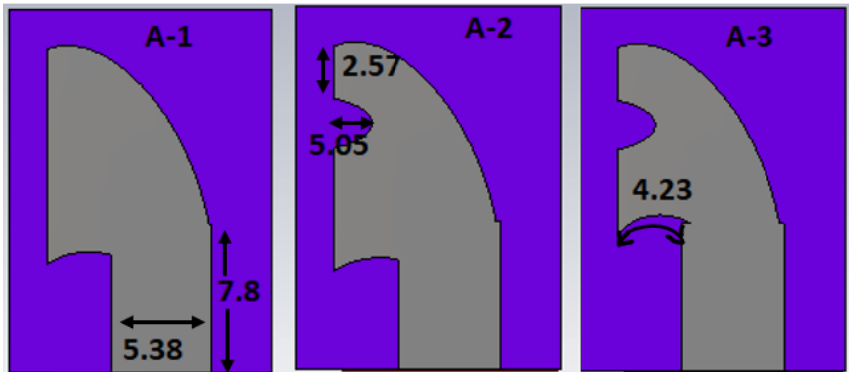

Figure 3. Single-element antenna design steps.

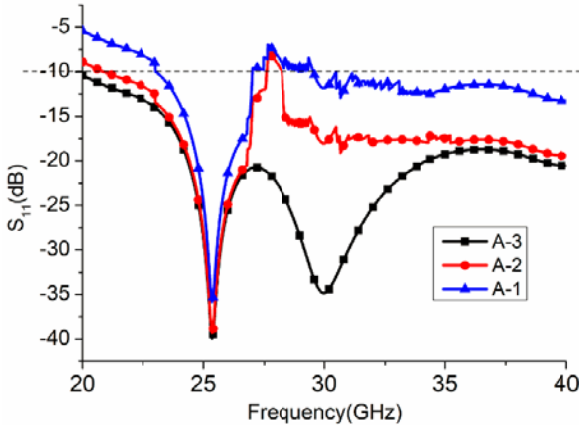

Figure 4. Simulated S_{11} plots of the single-element antenna design steps.

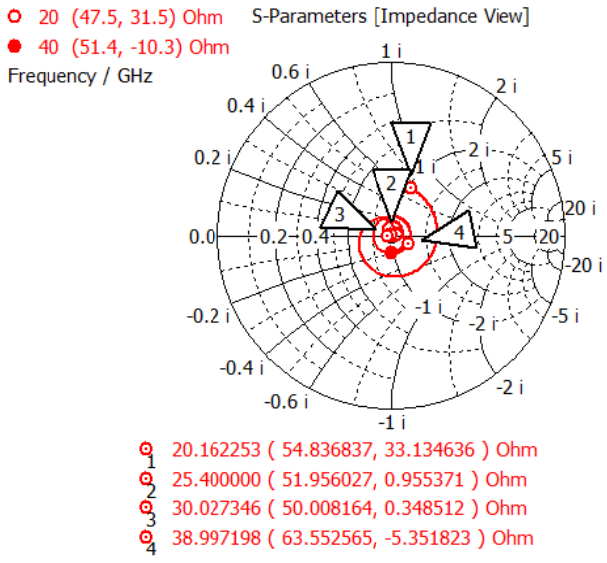

Figure 5. Simulated impedance matching (in smith chart) of the single-element antenna.

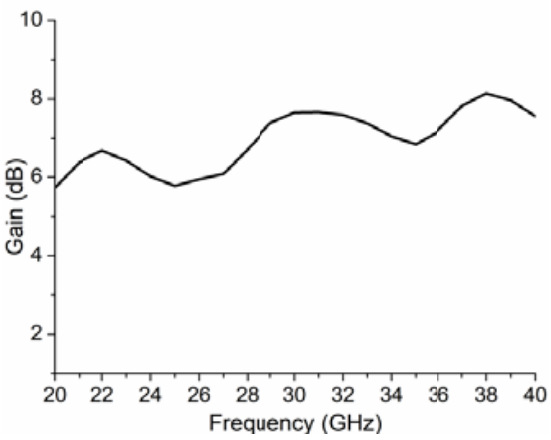

Figure 6. Simulated max gain over frequency (solid angle) plot of the single antenna.

which indicates an almost stable gain in the entire frequency range. The 2D simulated radiation plots of the suggested single-element design at 25.5 GHz, 28 GHz, 30 GHz, and 38 GHz are shown in Fig. 7.

2.2. Proposed Two Element MIMO Antenna Design

The single-element antenna design gives very good −10 dB impedance bandwidth results and 8.14 dB max gain in the frequency range of 20–40 GHz. With this optimized single-element design a 2 × 1 MIMO antenna is designed as shown in Fig. 8 configuration 1. The best-optimized separation between two elements is 11.2 mm (more than $\lambda/2$ for 25 GHz and above frequency), which provides more than −20 dB isolation in the entire frequency band.

The possible 2 × 1 MIMO antenna configurations' (1–4) schematic views are shown in Fig. 8. The simulated S parameters for return loss (S_{11}), isolation (S_{12}) for antenna element 1 and return loss (S_{22}), isolation (S_{21}) for antenna element 2 in the 20–40 GHz frequency band in graphical form for all possible configurations are shown in Figs. 9(a)–(d). The optimized dimension of the 2 × 1 MIMO antenna configuration 1 is $26 \times 19.2\,\text{mm}^2$. Fig. 9(a) shows good S-parameters in form of the return loss and low mutual coupling in form of the isolation for the entire 20–40 GHz frequency range. The simulated result shows that the antenna element 1 peak resonates at 25.5 GHz with a minimum return loss which is −52.18 dB, and the mutual coupling between the antenna elements is defined through the isolation parameter which is −21 dB. The antenna element 2 peak resonates at 27.8 GHz with a minimum return loss value of −66.5 dB, and isolation parameter S_{21} is −22.8 dB. The effectiveness or success of the designed 2 × 1 MIMO antenna system in terms of return loss, wide bandwidth, and isolation can be illustrated here.

Figures 9(b)–(d) show S-parameters in form of the return loss and mutual coupling in form of the isolation for the entire 20–40 GHz frequency range of MIMO configuration 2 to configuration 4. MIMO configuration 2 reflects the low mutual coupling between antenna element 1 and element 2. It also shows that S_{11} and S_{22} impedance parameters are not in agreements as shown in Fig. 9(b). MIMO antenna configuration 3 shows that S_{11} and S_{22} impedance parameters are almost same, but the mutual coupling between antenna elements is very low as indicated in Fig. 9(c). The last MIMO configuration 4 has good agreements between S_{11} and S_{22} impedance parameters, but the mutual coupling for the entire frequency band 20–40 GHz is not less than −20 dB as shown in Fig. 9(d) based on impedance parameters and mutual coupling analysis MIMO antenna. Configuration 1 is a perfect 2 × 1 MIMO antenna design for frequency band 20–40 GHz.

2.3. Mathematical Formula for Parametric Analysis

For quantitative analysis of the antenna parameters, some analytical formulas are used. They are computed using CST microwave simulation software. Some basic formulas are listed below.

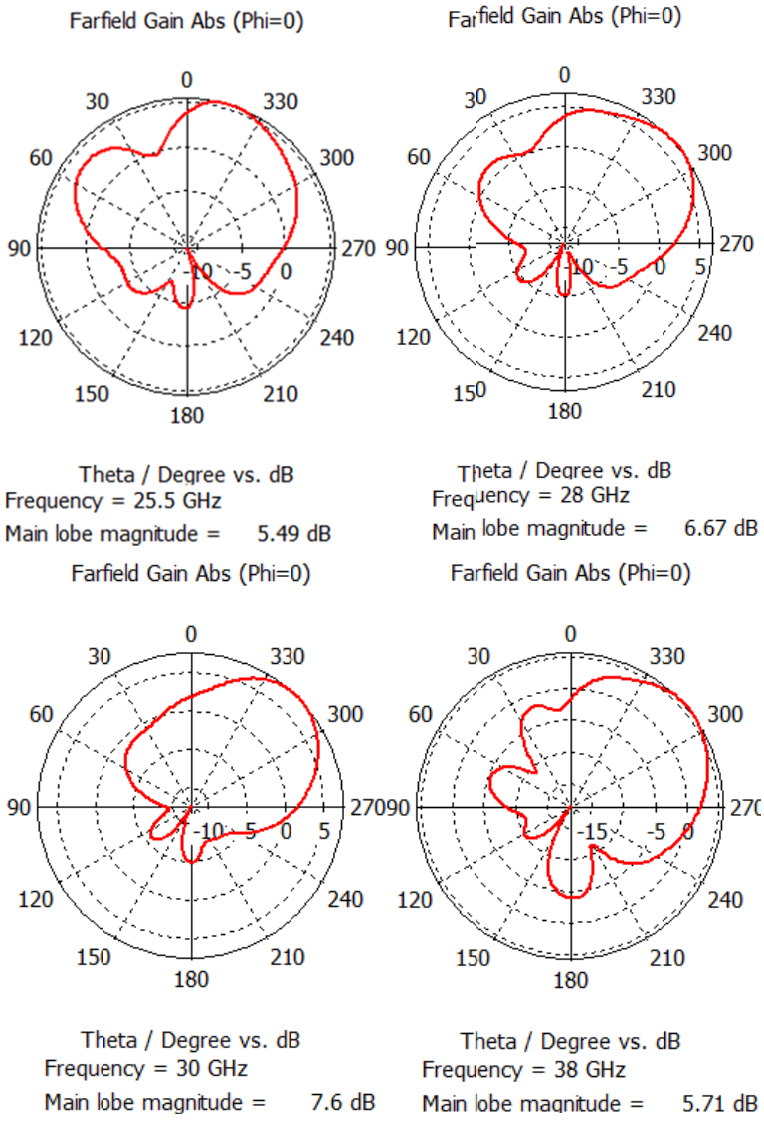

Figure 7. Simulated 2D radiation plots of the proposed single element antenna.

a. Return loss is $-66.5\,\text{dB}$, and the reflection coefficient of the proposed MIMO is found using Eq. (1) and Eq. (2) [12, 13].

$$R_l = -20\log_{10}|\text{Reflection coefficient}| \tag{1}$$

$$S_{11} = \frac{\text{the reflected voltage at port one}}{\text{the incident voltage at port one}} \tag{2}$$

b. Capacity and efficiency of any MIMO system are given by Eq. (3) and Eq. (4) [14]. The working efficiency of the proposed MIMO is above 85%.

$$C = \log_2\left|I + \frac{\rho}{n}HH^H\right| \tag{3}$$

I = identity matrix

n = no. of transmit antennas

H^T = conjugate transpose of the H matrix

ρ = correlation coefficient

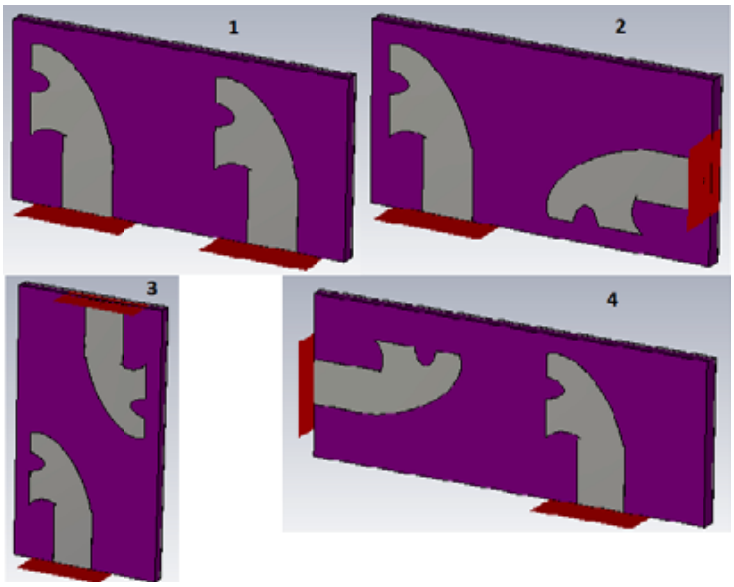

Figure 8. Schematic view of the proposed MIMO antenna configurations.

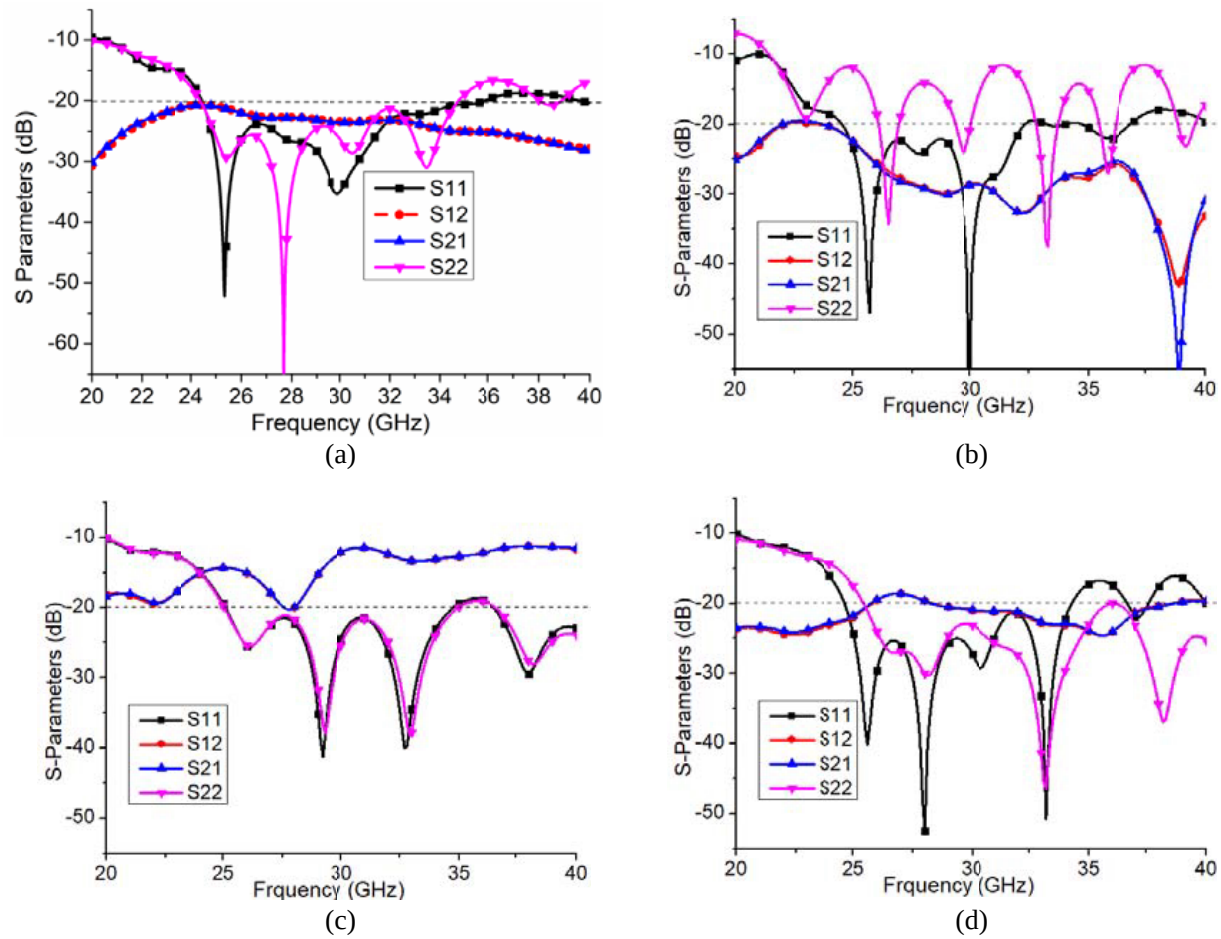

Figure 9. Simulated S-parameters of the 2×1 MIMO antenna configurations. (a) 2×1 MIMO antenna configuration 1. (b) 2×1 MIMO antenna configuration 2. (c) 2×1 MIMO antenna configuration 3. (d) 2×1 MIMO antenna configuration 4.

$$e_0 = e_r e_c e_d \tag{4}$$

where

e_0 = total efficiency

e_r = reflection efficiency

e_c = conduction efficiency

e_d = dielectric efficiency

c. Antenna gain is the quotient of power that radiates in a specified way to the power required for the isotropic radiator. The isotropic radiation intensity with the radiating power is identical to acceptable radiation power at the input separated via 4π that is an absolute gain of the antenna [15]. The formula for finding antenna gain is given by Eq. (5) [16], and the proposed MIMO gain is 8.17 dBi.

$$\text{Gain} = \frac{4\pi \times \text{radiation intensity}}{\text{Total radiated power}} \tag{5}$$

d. Envelope correlation coefficient (ECC) "ρe" illustrates the impact of the diverse transmission routes of the RF indicators in any MIMO antenna system [17]. The ECC is expressed in terms of S-parameters which is given by Eq. (6) [18], and the proposed MIMO ECC is 0.0001.

$$\rho e = \frac{\left|S_{11}^* S_{12} + S_{21}^* S_{22}\right|^2}{\left(1 - \left(|S_{11}|^2 + |S_{21}|^2\right)\right)\left(1 - \left(|S_{22}|^2 + |S_{12}|^2\right)\right)} \tag{6}$$

3. MIMO ANTENNA RESULTS

The fabricated prototype of the MIMO antenna is shown in Fig. 10, and Fig. 11 shows the prototype under testing. The simulated and measured S-parameters for the return loss (S_{11}) or reflection coefficient and isolation (S_{12}) for the 20–40 GHz frequency band are shown in graphical form in Figs. 12 and 13. The simulated result reflects that the peak resonates at 25.5 GHz with minimum return loss which is 48.5 dB, and the mutual coupling between the antenna elements is defined through the isolation parameter which is −23.10 dB. The measured return loss is −26 dB at 25.5 GHz in agreement with simulated one, and measured isolation is −23 dB which shows good agreement between them. From the

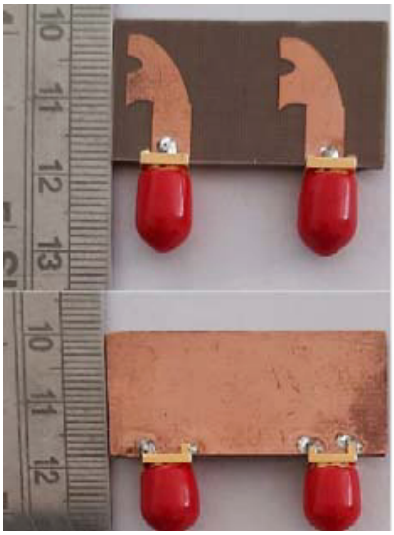

Figure 10. Fabricated MIMO antenna prototype.

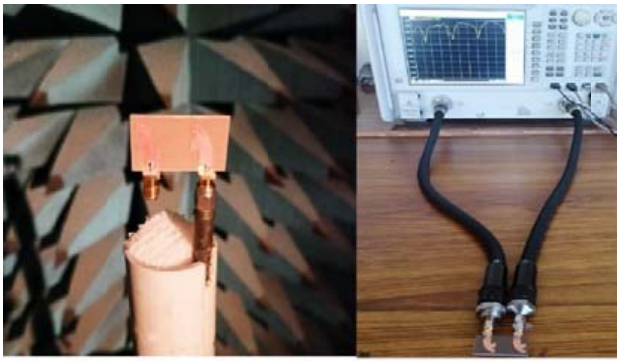

Figure 11. Antenna setup in anechoic chamber for testing.

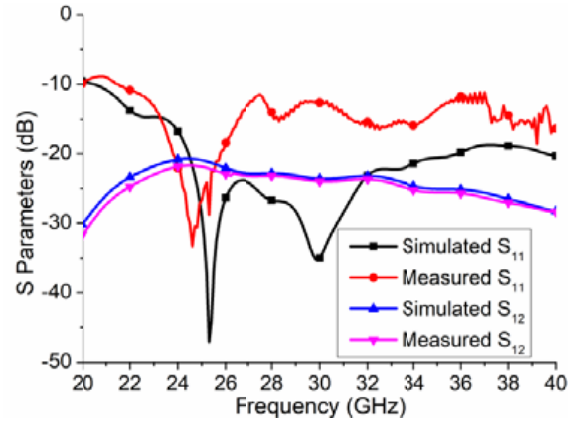

Figure 12. Simulated & measured S_{11}, S_{12} parameters.

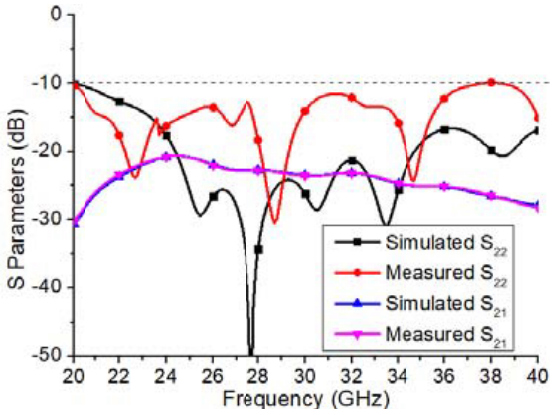

Figure 13. Simulated & measured S_{21}, S_{22} parameters.

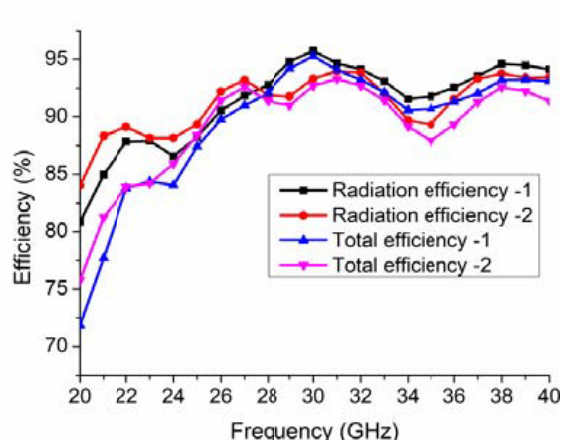

Figure 14. Simulated efficiency of designed MIMO antenna.

simulation results of S parameters, we find that S_{11} and S_{22} are less than -10 dB in the 20–40 GHz frequency band and the $S_{12} = S_{21}$ [19].

The S_{22} parameters are slightly different from S_{11} parameters. In MIMO antenna designs the radiating elements are closely proximate to achieve a compact design. The proximity of radiating elements and shared ground plane affects the antenna radiation performance.

The simulated radiation efficiency of the proposed MIMO antenna is shown in Fig. 14. Fig. 14 illustrates the radiation efficiency and total efficiency of antenna elements 1 and 2. Both the total and radiation efficiencies are more than 85% in the frequency band of 20–40 GHz.

The 2D simulated Fairfield radiation patterns for Phi = 0° and Phi = 90° for 25.5 GHz, 28 GHz, 30 GHz, and 38 GHz are shown in Fig. 15, Fig. 16, Fig. 17, and Fig. 18, respectively. From radiation plot, the result indicates that the suggested antenna is directional with the maximum gain in the upper half sphere at 25.5 GHz and 28 GHz. For 30 GHz and 38 GHz, the radiation is more directional due to an asymmetric patch design.

The simulated and measured gains over frequency plot are shown in Fig. 19 for the entire 20–40 GHz frequency band, which is more than 5.6 dBi, and the maximum gain is 8.17 dBi. The measured gain at 25.5 GHz is 5.01 dBi, and at 28 GHz it is 6.38 dBi. For 30 GHz, the gain is 7.01 dBi, and at 38 GHz measured gain is 7.78 dBi. The measured and simulated gains are almost the same. The suggested MIMO antenna has very good gain in the complete 20–40 GHz frequency band.

The envelope correction coefficient (ECC) involves all the S-parameters of the MIMO antenna, and it plays a key role as a radiating factor of the MIMO antenna system [20]. The simulated value of ECC is below 0.0001 as shown in Fig. 21 for the 23–32 GHz frequency band, and from 32–40 GHz it is below

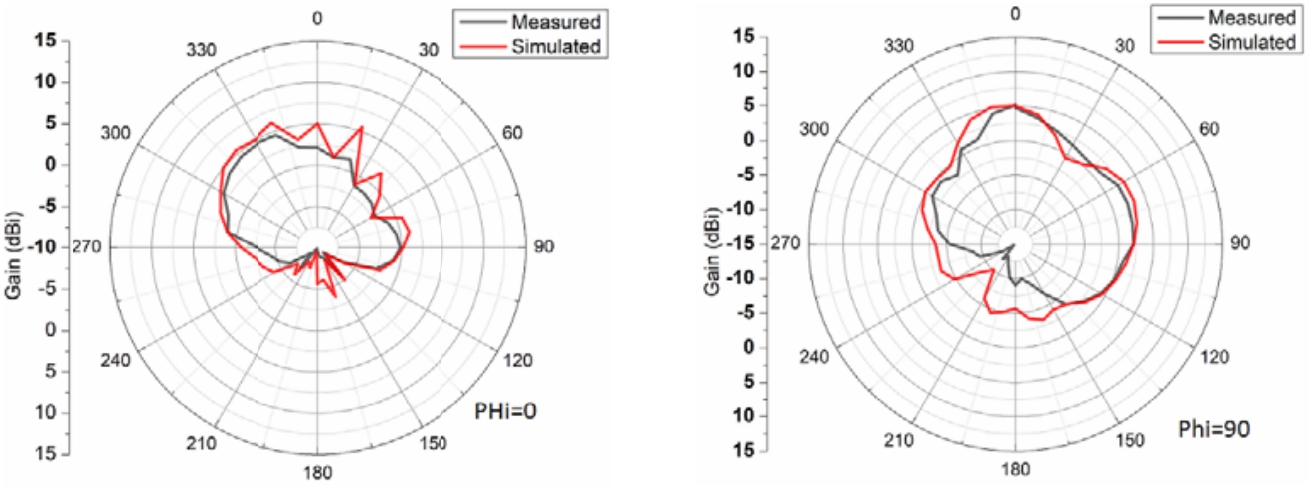

Figure 15. 2D radiation patterns at 25.5 GHz.

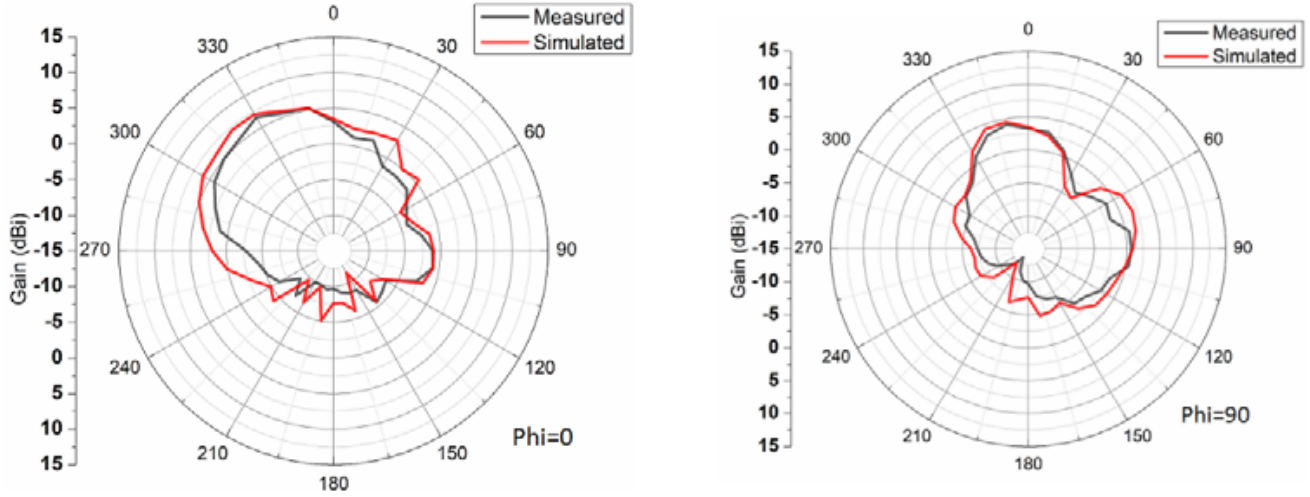

Figure 16. Simulated radiation patterns at 28 GHz.

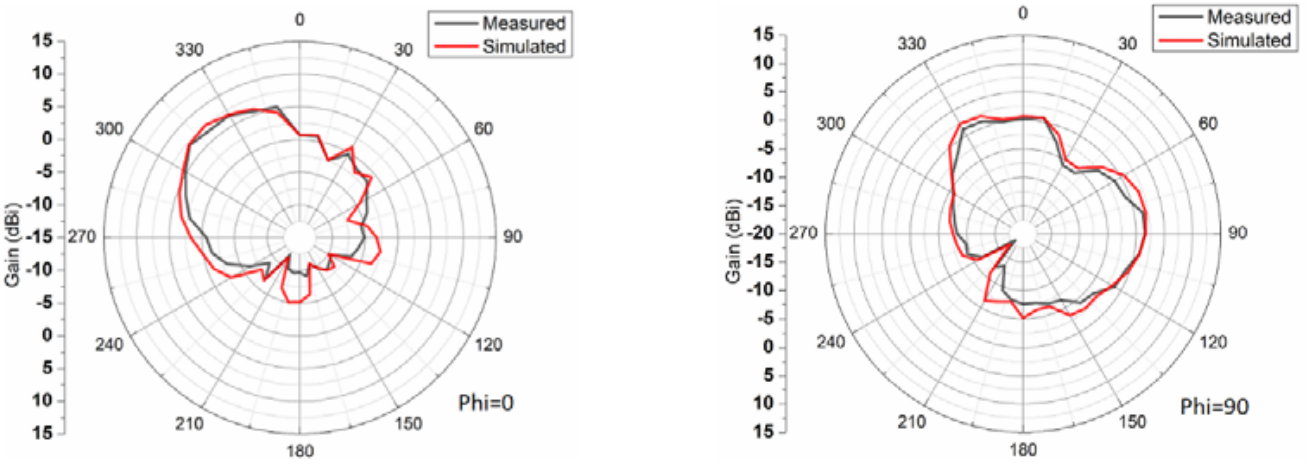

Figure 17. Simulated radiation patterns at 30 GHz.

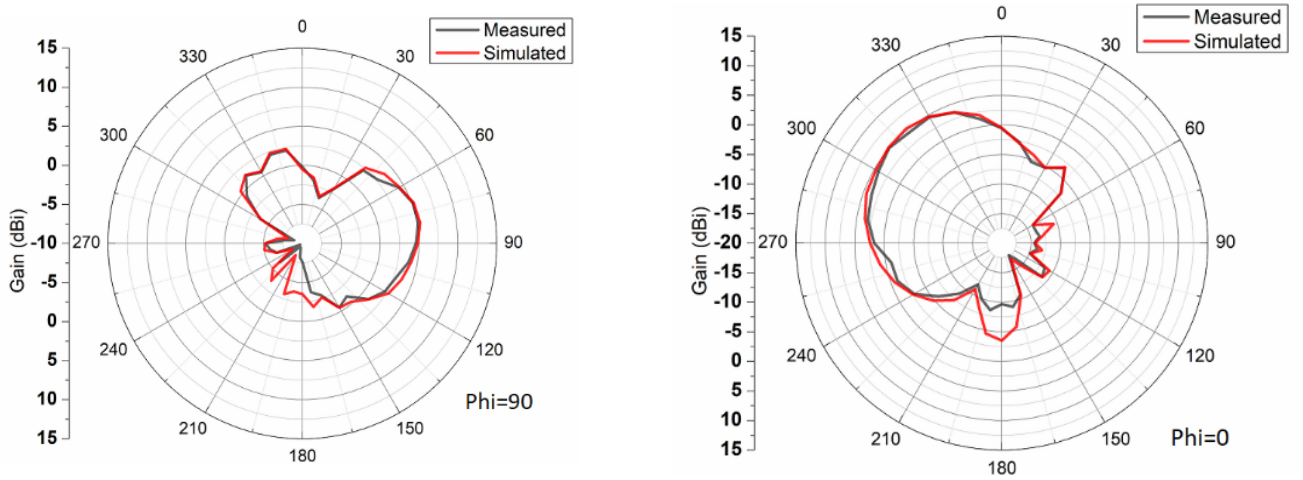

Figure 18. Simulated radiation patterns at 38 GHz.

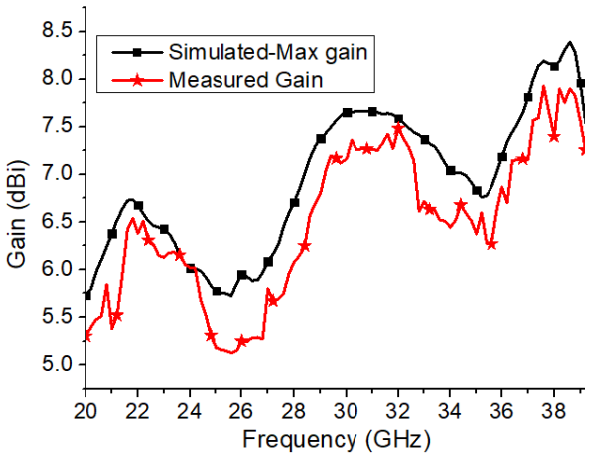

Figure 19. Simulated and measured gain over frequency.

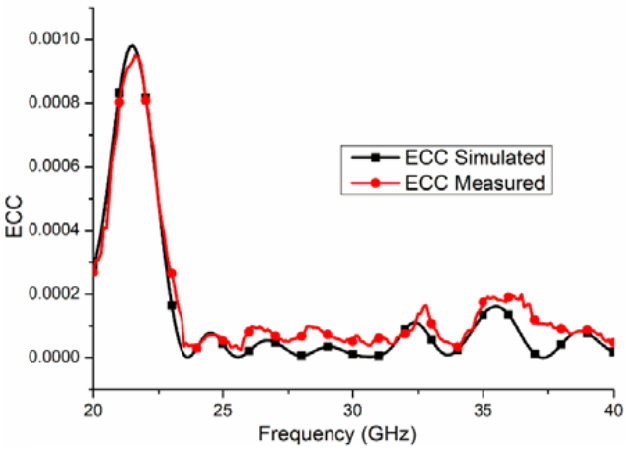

Figure 20. Simulated ECC of designed MIMO antenna.

Table 1. Comparison of the proposed work with previous work in literature review.

Parameter	R.6	R.7	R.8	Designed
Frequency (GHz)	24–36	26–40	26–40	20–40
Isolation (dB)	−20	−28	−24	−23.40
Return loss (dB)	−43	−28	−54	−48.5
Gain (dB)	7.5	8	9	8.17
ECC	0.005	-	0.02	< 0.0001
Size (mm^2)	126×126	60×135	24×22.5	26×19.2
Efficiency (%)	70	80	60	Above 85
material	Rogers 4003C	Isola	Rogers 5880	Rogers 5880

0.0002. The lower value of ECC justifies the lower correlation between MIMO antenna elements [21, 22].

It is observed that the suggested design provides good performance in terms of gain, efficiency, isolation, ECC, and return loss. Table 1 shows the comparison between results of the designed MIMO and other work.

4. CONCLUSION

The proposed two-element asymmetric flare shape MIMO antenna with 20 GHz to 40 GHz frequency band presents an efficient miniaturized system for Ka-band applications. It shows high bandwidth, low ECC, minimum return loss, and high isolation with good radiation characteristics. The proposed MIMO antenna design is compact and has more than 66.66% impedance bandwidth. The simulated minimum envelope correlation coefficient is 0.0001 which is very low and justifies the high isolation between antenna elements. The achieved isolation between antenna elements is more than 20 dB for the entire 20–40 GHz frequency band. The proposed antenna has demonstrated a high gain of 8.17 dBi with radiation efficiency above 85% in the operating range. The simulated and measured results of the proposed MIMO antenna are in good agreement. The distinguishing performance attributes of the designed MIMO antenna suggest its applications in the future 5G wireless networks and cellular applications of the millimeter wave communication.

REFERENCES

1. Malviya, L., R. K. Panigrahi, and M. V. Kartikeyan, "2 × 2 MIMO antenna for ISM band application," *11th International Conference on Industrial and Information System (ICIIS)*, 794–797, 2016.
2. Agarwal, A. and S. N. Mehta, "Design and performance analysis of MIMO-OFDM system using different antenna configurations," *International Conference on Electrical, Electronics, and Optimization Technique*, 1–5, 2016.
3. Madany, Y. M., R. A. Abdelrassoul, and N. Mohamed, "Miniaturized beam-switching array antenna with MIMO Direct Conversion Transceiver (MIMO-DCT) system for LTE and wireless communication applications," *Progress In Electromagnetics Research C*, Vol. 85, 9–23, 2018.
4. Agrawal, T. and S. Srivastava, "High gain microstrip MIMO antenna for wireless applications," *International Journal of Microwave and Optical Technology*, Vol. 12, 74–81, 2017.
5. Mohamed, Y. M., A. M. Dini, M. M. Soliman, and A. Z. M. Imran, "Design of 2 × 2 microstrip patch antenna array at 28 GHz for millimeter wave communication," *2020 IEEE International Conference on Informatics, IoT, and Enabling Technologies (ICIoT)*, 445–450, Doha, Qatar, 2020.
6. Wang, F., Z. Duan, X. Wang, Q. Zhou, and Y. Gong, "High isolation millimeter-wave wideband MIMO antenna for 5G communication," *International Journal on Antennas and Propagation*, 1–18, 2019.
7. Lee, W. W., I. J. Hwang, and B. Jang, "End-fire Vivaldi antenna array with wide fan-beam for 5G mobile handsets," *IEEE Access*, Vol. 8, 118299–18304, 2020.
8. Malviya, L., R. K. Panigrahi, and M. V. Kartikeyan, "Four element planar MIMO antenna design for long-term evolution operation," *IETE Journal of Research*, 1–7, 2017.
9. Patel, A., A. Vala, A. Desai, I. Elfergani, H. Mewada, K. Mahant, C. Zebiri, D. Chauhan, and J. Rodriguez, "Inverted-L shaped wideband MIMO antenna for millimeter-wave 5G applications," *Electronics*, Vol. 11, 1387, 2022.
10. Malviya, L., R. K. Panigrahi, and M. V. Kartikeyan, "MIMO antennas with diversity and mutual coupling reduction techniques: A review," *International Journal of Microwave and Wireless Technologies*, Vol. 9, 1763–1780, 2017.
11. Nadeem, I. and D. Y. Choi, "Study on mutual coupling reduction technique for MIMO antennas," *IEEE Access*, Vol. 7, 563–586, 2019.
12. Sharawi, M. S., "Printed multi-band MIMO antenna systems and their performance metrics," *IEEE Antennas and Propagation Magazine*, Vol. 55, 220–232, 2013.
13. Sharawi, M. S., A. B. Numan, and D. N. Aloi, "Isolation improvement in a dual-band element MIMO antenna system using capacitively loaded loops," *Progress In Electromagnetics Research*, Vol. 134, 247–266, 2012.

14. Paliwal, H. P. and N. Agrawal, "Dumb-bell shaped defected ground structures MIMO antenna for UWB applications," *11th IEEE International Conference on Communication Systems and Network Technologies*, 42–48, 2022.
15. Liu, H., W. Yang, A. Zhang, S. Zhu, Z. Wang, and T. Huang, "A miniaturized gain-enhanced antipodal Vivaldi antenna and its array for 5G communication applications," *IEEE Access*, Vol. 6, 76282–76288, 2018.
16. Paliwal, H. P., "Design and analysis of E shaped microstrip patch antenna with defected ground structure for improvement of gain and bandwidth," *International Conference on Optical & Wireless Technologies, MNIT Jaipur*, 195–202, 2020.
17. Honma, N. and K. Murata, "Correlation in MIMO antennas," *Electronics (MDPI)*, Vol. 9, 1–16, 2020.
18. Paliwal, H. P. and N. Agrawal, "Design of polarized 2×2 MIMO antenna using partially stepped ground," *International Conference on Optical & Wireless Technologies, MNIT Jaipur*, 181–188, 2020, ISBN 978-981-16-2818-4 (eBook).
19. Paliwal, H. P. and N. Agrawal, "A 2×1 dual-band MIMO antenna using complementary split ring resonator for wireless applications," *TEST Engineering and Management*, Vol. 82, 111212–11216, 2019.
20. Paliwal, H. P. and N. Agrawal, "Design of circularly polarized MIMO antenna using defective ground structure for wireless applications," *IJIRCCE*, Vol. 8, No. 6, 2159–2163, June 2020.
21. Tu, D. T. T., N. V. Hoc, P. D. Son, and V. V. Yem, "Design and implementation of dual-band MIMO antenna with low mutual coupling using electromagnetic band gap structures for portable equipment," *International Journal of Engineering and Technology Innovation*, Vol. 7, 48–60, 2017.
22. Niu, Y., Y. Li, D. Jin, L. Su, and A. V. Vasilakos, "A survey of millimeter wave (mmWave) communications for 5G: Opportunities and challenges," *Wireless Networks*, Vol. 21, No. 8, 1–17, 2015.